Date of publication xxxx 00, 0000, date of current version xxxx 00, 0000.

Digital Object Identifier 10.1109/ACCESS.2017.DOI

Advancements In Spectral Power Distribution Modeling Of Light-Emitting Diodes

S. BENKNER[1], A. HERZOG[1], S. KLIR[1], W.D. VAN DRIEL[2], AND T. Q. KHANH[1]

[1]Technical University of Darmstadt, Laboratory of Adaptive Lighting Systems and Visual Processing, 64289 Darmstadt, Germany (e-mail: benkner@lichttechnik.tu-darmstadt.de)

[2]Delft University of Technology, Electronic Components, Technology and Materials, Faculty of Electrical Engineering, Delft, The Netherlands

Corresponding author: S. Benkner (benkner@lichttechnik.tu-darmstadt.de).

ABSTRACT The unique radiative, photometric and colorimetric characteristic of a light-emitting diode is derived from its spectral power distribution. Modeling such characteristics with respect to the forward current, temperature or operating time has been subject of various studies. Deriving a simple analytical model, however, is not trivial due to the unique emission pattern varying with different types and technologies of light emitting diodes. For this purpose, curve fitting multiple superimposed Gaussian probability density functions to the spectral power distribution is a common approach. Despite very a high R^2 goodness of fit results, significant deviations within the photometric and colorimetric parameters, such as luminous flux or chromaticity coordinates, are observed. In addition, most studies were conducted on a small sample set of very few different spectral power distributions. This work provides a comprehensive comparison and evaluation of 19 different (superimposed) probability density function based models provided by the literature tested on a total of 15 different spectral power distributions of monochromatic blue, green and red light-emitting diode as well as phosphor-converted spectra of lime, purple and different correlated color temperature types white samples. All models were evaluated by means of their coefficient of determination, radiant flux, chromaticity coordinate deviation and Bayesian Information Criterion. This study shows that a superimposed (split) Pearson VII model is able to outperform the commonly used Gaussian model approach by far. In addition, an application example in regard of forward current dependence is given to prove the proposed approach.

INDEX TERMS light-emitting diode, LED, spectral power distribution, spectral modeling, spectral decomposition

I. INTRODUCTION

The emission pattern of a light-emitting diode (LED) can be described by its spectral power distribution (SPD) $S(\lambda)$. Typical performance metrics such as the radiant and luminous flux Φ_e, Φ_v, CIE color coordinates, Correlated Color Temperature (CCT) or the Color Rendering Index (CRI) are derived from the SPD [1]. The shape of $S(\lambda)$ is formed by two main factors: First, the material parameters of the LED such as semiconductor material, number of quantum wells or the type of phosphor in case of a phosphor-converted (pc-)LED. Secondly, operating conditions impact the SPD by means of Drive Current I_F, Junction Temperature T_j, Ambient Temperature T_A, Humidity $\mathbf{r}H_A$ and operating time t. In order to investigate the influence of a specific material or operating parameter the SPDs behavior is modeled by means of this parameter. A popular modeling approach is deconvoluting the SPD in separate SPDs $S(\lambda) = \sum S_n(\lambda)$, such as $S_{\text{Chip}}(\lambda) + S_{\text{Phosphor}}(\lambda)$ for pc-LEDs. Using a superposition of probability density functions (pdf) $S_n(\lambda) = f_{pdf}(x = \lambda)$ is a commonly used approach. Each separated SPD can then be further analyzed for example regarding its chromaticity shift and direction to identify underlying degradation mechanisms [2] .Real world SPD, however, exhibit pdf shapes with a certain skew. This either produces inaccuracies for a low number $S_n(\lambda)$ or resulting in an impractical high number of pdfs to ensure a certain accuracy.

The aim of this work is on finding a proper set of model functions for modeling the SPD of various monochromatic and pc-LEDs. Therefor, a review on existing modeling approaches is given. Afterwards a set of suitable model func-

This article has been accepted for publication in IEEE Access. This is the author's version which has not been fully edited and content may change prior to final publication. Citation information: DOI 10.1109/ACCESS.2022.3197280

tions is evaluated on seven monochromatic and six pc-LEDs. Subsequently the results are discussed and the optimized model function is implemented for an application example on simulating a monochromatic LEDs current dependency.

II. RELATED WORK

A. MONOCHROMATIC LED SPECTRA

The theoretical emission spectrum $I(E)$ of a monochromatic LED [3] is described by the product of the density of states $\rho(E)$ and carrier distribution allowed in the energy band described by the Boltzmann distribution $f_B(E)$ given in (1) with the Energy E, the Bandgap Energy E_g, Temperature T and Botzmann constant k_B .

$$I(E) \propto \rho(E) \cdot f_B(E) = \sqrt{E - E_g} \cdot e^{\frac{-E}{k_B T}} \tag{1}$$

Modeling the SPD by (1) requires in depth knowledge about the LEDs material parameters. Even then, due to variations in the manufacturing process and material composition as well as the physical construction of the LED package, it is difficult to give a sufficient estimate of the SPD. Reifegerste et al. [4] in 2008 proposed the idea of modeling a monochromatic LEDs spectral shape at different I_F and T_j by curve fitting different analytical functions to the SPD. For this purpose a set of ten functions were investigated on a single LED type. The functions are listed in table 2. It was concluded that a *Logistic Power Peak* model performed best on the studied LED sample. Contrary in [5] best results were yielded for an Asymmetric Double Sigmoidal (*Asym2Sig*) models on a blue, green and red LED sample. Keppens et al. [6] evaluated a Sum of *Gaussian* model on each two red, green and blue LED samples reporting a high coefficient of determination $R^2 > 0.97$ for five out of six LED samples. This study was extended with amber and red samples by Raypah et al. [7] reporting $R^2 > 0.95$. By approximating (1) with an infinite series expansion of *Power Law* model functions for both sides of the peak wavelength λ_p Mozyrska and Fryc [8] took a different approach. A $R^2 \approx 0.98$ could be realized on a deep blue $380\,\mathrm{nm}$ sample with a $R^2 \approx 0.99$ on a *Gaussian* model for as comparison. Current LEDs often utilize a multi quantum well (MQW) structure impacting the SPDs slope. For this purpose Vaskuri et al. [9], [10] reported suitable results for red and blue samples utilizing an *Asym2Sig* model. Since the scope of their work was on modeling junction temperatures no goodness of fit metrics were provided for a comparison to the studies above.

B. PHOSPHOR-CONVERTED LED SPECTRA

Analogous to monochromatic LEDs over the past decade advances in modeling pc-LEDs were reported. The following studies present exclusively white pc-LEDs since modeling color pc-LEDs (purple, amber, green/lime) have not been the scope of any study yet. A number of results on Sum of n *Gaussian* models with $n = 2..8$ superimposed pdfs have been reported. Guo et al. [11] separated the SPD in two narrow band (blue, red) and one wide band region (green). Subsequently, each region was modeled with two (narrow band) respectively four (wide band) totaling $n = 8$ weighted *Gaussian* model functions but no R^2 was reported. Similarly a combination of $n = 7$ unweighted *Gaussian* model was chosen by a R^2-maximizing algorithm by Song and Han [12]. On an $n = 2$ unweighted *Gaussian* model Chen et al. [13] achieved a $R^2 > 0.99$ on four different samples. Additional, [14]–[17] focus on predicting certain performance parameters of white pc-LEDs by incorporating *Gaussian* models in their prediction algorithms denoting $R^2 > 0.98$ for the input fitting functions. Fan et al. yielded in their model SPD a minimal higher coefficient of determination for the *Asym2Sig* model compared to the *Gaussian* model of both $R^2 \approx 0.99$.

C. PHOTOMETRIC AND COLORIMETRIC ACCURACY VS. COEFFICIENT OF DETERMINATION

The majority of the above mentioned studies present the coefficient of determination as a proper evaluation metric. From a mathematical or statistical point of view a $R^2 > 0.95$ may indicate a high correlation and thus a good result. Nonetheless some studies yield at best moderate results in the radiometric or colorimetric domain [5]–[7], [11], [15], [17], [18]. Therefor, a combination of statistical, colorimetric and radiometric parameters should be taken into account when selecting a proper model function.

III. EXPERIMENT

The following section emphasizes on describing the experimental details in regard of LED samples used, the investigated model functions and the implementation.

A. SAMPLES

A total of 15 different monochromatic (blue, green, red) and pc-LEDs (lime, purple, white) were selected to cover a diverse spectral range of SPDs within the visible light spectrum. Table 1 highlights the most important radiometric and colorimetric parameters. It should be noted, that the peak wavelengths for plateaus in the SPD were estimated to point out a distinct underlying function. The normalized SPDs are shown in Fig. 1.

B. IMPLEMENTATION

The experimental code is implemented in Python programming language with the LMFIT package [19] for model fitting and evaluation. For this purpose the built-in set of model functions was extended by custom models according to the literature. Table 2 gives an overview of the evaluated models $f(\lambda, p)$ with their set independent variables $p = \{p_1, ...p_n\}$ as well as the literature reference for the model implementation. It should be noted, that two varying Pearson type VII models were found in the literature. Therefor, both implementation by Reifegerste et al. [4] and LMFIT built-in [19] are denoted Pearson VIIa and Pearson VIIb respectively. The common model parameter boundaries were arbitrarily set to the following intervals: Amplitude $A \in [0.001, 100]$, Peak Wavelength $\lambda_p \in [400, 800]$, (left/right side) Standard

TABLE 1. Overview of LED sample key parameters: Radiant Flux Φ_e, Peak Wavelength(s) λ_{pn}, CIE 1976 USC u', v'.

Sample	Φ_e (mW)	λ_{pn} (nm)	u' (a.u.)	v' (a.u.)
Blue 1	306.4	450.6	0.203	0.079
Blue 2	290.5	445.9	0.215	0.061
Blue 3	550.2	444.6	0.218	0.058
Green	184.7	518.9	0.054	0.571
Red 1	177.3	632.4	0.533	0.520
Red 2	336.5	633.4	0.537	0.519
Red 3	367.8	660.0	0.587	0.512
Lime	245.5	447.8; 541.1	0.187	0.558
Purple	363.3	447.6; 646.2	0.463	0.503
White 1	470.3	443.5; 515.7; 550.5; 650.9	0.220	0.482
White 2	214.6	443.3; 597.5	0.229	0.507
White 2700K	333.6	449.0; 461.7; 626.4	0.267	0.533
White 3000K	320.4	450.0; 461.6; 623.1	0.253	0.533
White 4000K	379.9	443.0; 547.0; 616.8	0.225	0.511
White 6500K	374.3	442.3; 536.1; 614.3	0.197	0.482

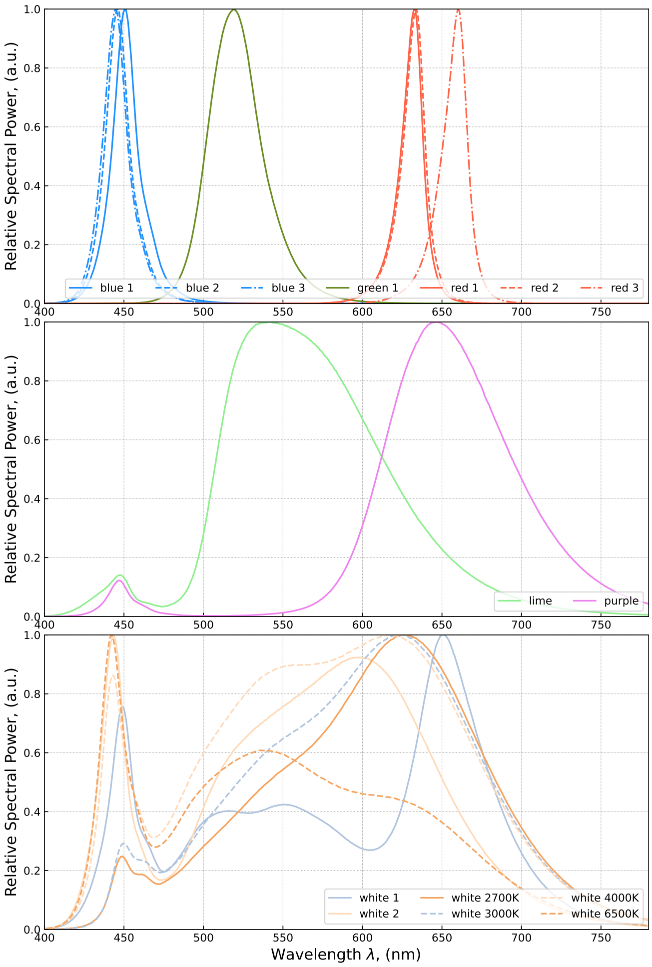

FIGURE 1. Peak wavelength intensity normalized test spectra of 13 sample LEDs: (top) monochromatic spectra of three blue, three red and one green LED; (bottom) phosphor-converted spectra of four white, one lime and one purple LED.

Deviation $\sigma, \sigma_1, \sigma_2 \in [1, 300]$. Additional model specific parameter intervals can be found in table 2. All code is available at our repository: *https://github.com/SBenkner/Spectral-Fitting*.

TABLE 2. Evaluated model functions for the experiment with their fitting parameters and the models literature reference.

Model	Independent Variables	Source
Gaussian	A, λ_p, σ	[4]–[8], [11]–[21]
Split Gaussian	$A, \lambda_p, \sigma_1, \sigma_2$	[4], [5]
Exponential Gaussian	A, λ_p, σ $\gamma \in [-100, 100]$	[19]
Skewed Gaussian	A, λ_p, σ $\gamma \in [-100, 100]$	[19]
Lorentzian 1. Ord.	A, λ_p, σ	[15], [16], [19]
Split Lorentzian 1. Ord.	$A, \lambda_p, \sigma_1, \sigma_2$	[19]
Lorentzian 2. Ord.	A, λ_p, σ	[4]
Asym. 2 Sigmoidal	A, λ_p, σ $S_1, S_2 \in [10^{-15}, 100]$	[4], [5], [9], [10], [16], [21]
Logistic Power Peak	A, λ_p, σ $S \in [10^{-15}, 100]$	[4], [5]
Asym. Power Peak	A, λ_p, σ $S \in [10^{-15}, 100]$	[4]
Pearson VIIa	A, λ_p, σ $S \in [10^{-15}, 100]$	[4]
Pearson VIIb	A, λ_p, σ $m \in [10^{-15}, 100]$	[19]
Split Pearson VII	$A, \lambda_p, \sigma_1, \sigma_2$ $S_1, S_2 \in [10^{-15}, 100]$	[4]
Voigt	A, λ_p, σ $\gamma = \sigma$	[19]
Pseudo Voigt	A, λ_p, σ $\alpha \in [10^{-15}, 100]$	[19]
Skewed Voigt	A, λ_p, σ $\gamma = \sigma$ $S \in [10^{-15}, 100]$	[19]
Moffat	A, λ_p, σ $\beta \in 10^{-15}, 100]$	[19]
Student T	A, λ_p, σ	[19]
Lognormal	A, λ_p, σ	[19]

Independent Variables: Amplitude A; Peak Wavelength λ_p; (left/right side) Standard Deviation $\sigma, \sigma_1, \sigma_2$; (left/right side) Skew/Kurtosis S, S_1, S_2; weighting or scaling parameter α, β, γ, m.

Preliminary, two assumptions are made to find the most suitable fit function: The radiation pattern of a monochromatic LED follows only one type of model function. This function type can be superimposed $n_{\text{Chip}} \geq 1$ times to represent e.g. n different QW in a MQW structure. Secondly, pc-LEDs incorporate at least two superimposed functions $n = n_{\text{Chip}} + n_{\text{Phosphor}} \geq 2$ where $n_{\text{Chip}} \geq 1$ and $n_{\text{Phosphor}} \geq 1$. Since it can be assumed that $\lim_{n\to\infty} R^2 \to 1$ the number of model functions is limited to $n = 3$ for monochromatic LEDs and $n = 6$ for pc-LEDs to maintain a realistic and practical approach. Thus, with the given constraints the total number of possible model combinations can be calculated with $N(n) = M \cdot \sum_i^n i$ to $N_{\text{mono}}([1,3]) = 57$ and $N_{\text{pc}}([2,6]) = 95$ with $M = 19$ different model functions. The maximum number of fit iterations before the fit is aborted is set to 100.000. Each fit is evaluated regarding its statistical, radiometric and colorimetric properties. In order to provide a comparability to the literature the coefficient of determination R^2 (2) has been selected from the statistical domain. Additionally, the fitted models Bayesian Information Criterion (BIC) was determined according to (3) with the number of data points m, the number of parameters k and the models maximum likelihood function $\hat{L}$ [22]. From the radiometric domain the relative difference in radiant flux $\Delta\Phi$ (4) was evaluated since even changes in brightness of about 7.4% are noticeable according to Hu and Davis [23]. To accompany a steadiness in the colorimetric perception the chromaticity difference $\Delta u'v'$ (5) [1] was chosen from the colorimetric domain since the CIE 1976 $u'v'$ color space is recommended by the CIE for its uniformity [24].

$$R^2 = \frac{\sum(y_{\text{i,fit}} - \bar{y}_{\text{true}})^2}{\sum(y_{\text{i,true}} - \bar{y}_{\text{true}})^2}, \bar{y}_{\text{true}} = \frac{\sum_i^m y_{\text{i,true}}}{N} \tag{2}$$

$$\text{BIC} = k\ln(m) - 2\ln(\hat{L}) \tag{3}$$

$$\Delta\Phi = 100 \cdot \left(\frac{\Phi_{\text{fit}}}{\Phi_{\text{true}}} - 1\right) \tag{4}$$

$$\Delta u'v' = \sqrt{(u_{\text{fit}} - u_{\text{true}})^2 - (v_{\text{fit}} - v_{\text{true}})^2} \tag{5}$$

In order to delimit the set of possible models boundaries have to be set for each evaluation metrics (2)-(5) to rule out irrelevant models. Since, the coefficient of determination shows the correlation between the original and its fitted SPD a $R^2 \geq 0$ has to be expected. Values $R^2 < 0$ would indicate a negative correlation yielding an inverse shaped SPD fit of the original SPD. A difference in radiant flux of $\Delta\Phi < -100\%$ would represent a physically impossible negative SPD. Due to the high sensitivity of the human eye regarding a change of brightness the range of allowed difference in radiant flux was arbitrarily set to $\Delta\Phi \pm 25\%$. Considering the CIE 1976 UCS color space boundaries chromaticity difference values above $\Delta u'v' \approx 75 \times 10^{-3}$ would exceed the spectral locus. As described in [24] thresholds for $\Delta u'v'$ are mainly defined near the Planckian Locus of the CIE 1976 UCS color space diagram it is difficult to chose a specific threshold especially for monochromatic spectra. Thus, in this work the *CS4* threshold declared in IES/ANSI TM-35 [25] of $\Delta u'v' = 4 \times 10^{-3}$ is used.

IV. RESULTS AND DISCUSSION

Following, the different fit models results are presented and discussed with respect to their accuracy according to (2)-(5). First the results of the monochromatic set of SPDs are evaluated. Subsequently, the set of pc-LED spectra is analyzed.

In case of the monochromatic SPD samples 399 theoretical models in total were evaluated. Considering the above defined constraints a total of 174 models remained as valid for further inspection. Table 3 shows the number of valid functions for each sample and number of superimposed functions. As previous stated, the accuracy, and thus the number of valid models, increases with n. It can also be concluded that even with $n = 1$ at least one model function can be found meeting the boundary conditions. Superimposing at least two functions yields a $\Delta u'v' < 2 \times 10^{-3}$ for all valid models.

Next, the top ten models with the lowest $\Delta u'v'$ of each sample SPD were compared. According to majority of the literature a composition of *Gaussian* models was expected to yield the best results. However, on the given monochromatic sample SPDs the *Gaussian* model was vastly underrepresented. A *(split) Pearson VII* distribution and *Skewed Voigt* model provided the lowest $\Delta u'v'$ and $\Delta\Phi$. The information gain from the coefficient of determination was rather small since all selected models showed a $R^2 \geq 0.98$. Taking $\Delta\Phi$ and BIC into account *(split) Pearson7* performed best overall on all monochromatic samples. It should be noted, that in most cases the LMFIT implemented *Pearson VIIb* model [19] performed best, yet all three *Pearson VII* models yielded superior results. A comparison of the *Pearson VII* and the *Gaussian* models for different n is given in table 4 and 5 for $\Delta u'v'$ and $\Delta\Phi$ respectively. In case of the red samples with a $n = 1$ *Gaussian* model the fit process exceeded the maximum fit iterations probably due to the chosen parameter boundaries in combination with the SPDs high right side skew an steep decrease. Therefore, no values can be reported. With only one *Pearson VII* type function 5 of 7 samples could meet the *CS4* condition while the remaining two samples slightly failed it by $\Delta u'v' < 0.51 \times 10^{-3}$. Whereas for the *Gaussian* models exceeded $\Delta u'v' < 10 \times 10^{-3}$. Even with $n = 3$ only 3 of 7 samples matched the *CS4* condition for the *Gaussian* model. An observable increase in $\Delta u'v'$ and $\Delta\Phi$ for $n = 2$ on sample Red 3 can be traced to a problems fitting two functions on the given type of SPD decreasing the fit quality compared to $n = 1$ due to *Gaussian* models missing kurtosis parameters.

A similar procedure was performed for evaluating the pc-

TABLE 3. Total number of valid models for each sample and number of functions n.

Sample	$n=1$	$n=2$	$n=3$	$n=4$	$n=5$	$n=6$
Blue 1	1	2	9	-	-	-
Blue 2	5	6	12	-	-	-
Blue 3	5	6	12	-	-	-
Green	5	9	11	-	-	-
Red 1	1	3	10	-	-	-
Red 2	1	5	9	-	-	-
Red 3	2	3	8	-	-	-
Lime	-	5	11	12	13	12
Purple	-	0	0	5	8	7
White 1	-	0	7	6	10	11
White 2	-	9	14	13	11	14
White 2700K	-	10	14	14	15	14
White 3000K	-	6	14	14	14	12
White 4000K	-	3	12	10	10	11
White 6500K	-	5	10	12	13	15

TABLE 4. Chromaticity difference results of Pearson Type VII distribution (P7) compared to Gaussian distribution (G) with $n = 1..3$ model functions on the monochromatic LED set.

LED	$\Delta u'v'$ ($\times 10^{-3}$)					
	n=1		n=2		n=3	
	P7	G	P7	G	P7	G
Blue 1	4.04	16.78	1.00	8.88	1.21	5.06
Blue 2	0.73	12.08	2.38	5.99	0.51	4.75
Blue 3	1.44	11.54	2.00	5.79	0.32	4.62
Green	1.17	10.02	0.41	1.56	0.05	0.19
Red 1	2.55	-	2.20	7.32	0.07	2.51
Red 2	0.37	-	2.54	6.87	0.28	2.49
Red 3	4.51	-	10.15	16.93	0.37	3.53

TABLE 5. Difference in radiant flux results of Pearson Type VII distribution (P7) compared to Gaussian distribution (G) with $n = 1..3$ model functions on the monochromatic LED set.

LED	$\Delta\Phi$ (%)					
	n=1		n=2		n=3	
	P7	G	P7	G	P7	G
Blue 1	2.6	-8.1	-0.1	-1.4	0.0	-0.9
Blue 2	1.5	-7.5	0.4	-1.0	0.0	-1.0
Blue 3	1.2	-6.9	-0.3	-0.8	0.0	-0.9
Green	0.1	-3.8	0.1	-0.7	0.1	-0.2
Red 1	1.0	-	0.6	-2.0	0.1	-0.4
Red 2	1.3	-	0.7	-1.8	0.1	-0.4
Red 3	0.6	-	0.9	-7.8	-0.1	-0.4

LED spectra. Out of the 760 evaluated models 406 models met the boundary conditions. Due to the varying shape of the phosphor-related spectral emissions a broader set of possible functions could be identified: *Gaussian*, *Split Gaussian*, *Skewed Gaussian*, *Asym2Sig*, *Pearson VIIa/b*, *Split Pearson VII*, *Skewed Voigt* and *Moffat*. The total number of valid functions for the pc-LED SPDs with respect to the number of superimposed functions is shown in fig. 3. Apart from the Purple and White 1 sample it was possible to find at least one model that met the *CS4* condition at $n = 2$ on every sample. Since White 1 was explicitly chosen because of its three phosphor peaks it was expected to fail. The purple sample on the other hand could not be fitted properly with low n two separated peaks as further described at the end of this passage. In accordance to the monochromatic results described above the *(Split) Pearson VII* on average on all samples again yielded promising results as shown in tables 6 and 7. Especially at lower model numbers $n \leq 3$ *(Split) Pearson VII* outperforms a *Gaussian* model approach by a factor of at least more than two. Yet, with only two superimposed functions 5 of 8 samples can be sufficiently modeled with a *(Split) Pearson VII* model compared to only 1 of 8 models meeting the *CS4* condition with a *Gaussian* model. At higher model number of $n \geq 4$ both model types perform with a high accuracy. Further two special cases are observable: Firstly, the Purple and White 4000K samples show an increase in $\Delta u'v'$ at $n = 6$ and $n = 5$ respectively for the *Gaussian* model that can be traced back to fitting problems analogous to the Red 3 sample. Secondly, both model types produce a high chromaticity difference for the Purple sample at $n = 2, 3$. This situation occurs mostly due to the fact, that the fitting algorithm has to find a trade-off between magnitude and width of the resulting function alongside with a desired shape. For the given model types either the magnitude requirement is met by overfilling the valley between since the functions width exceeds the peak width. Alternatively, one or both peaks are underfilled since the shape/width requirements are satisfied with the drawback in magnitude.

The observed improvements of a *Pearson VII* compared to *Gaussian* type model can be concluded due to two reasons: *(Split) Pearson VII* provides additional shape/skew adjustment capabilities given by its exponents m, S, S_1 and

TABLE 6. Chromaticity difference results of Pearson Type VII distribution (P7) compared to Gaussian distribution (G) with $n = 2..6$ model functions on the pc-LED set. The following abbreviations are used for the sample: W1=White 1, W2=White 2, WxxK=White xx00K.

LED	$\Delta u'v'$ $(\times 10^{-3})$									
	n=2		n=3		n=4		n=5		n=6	
	P7	G	P7	G	P7	G	P7	G	P7	G
Lime	1.01	6.43	0.03	6.01	0.03	2.79	0.23	0.02	0.03	0.01
Purple	12.5	29.93	6.83	29.27	0.12	2.37	0.05	1.17	0.17	21.37
W1	6.07	25.61	1.18	0.84	0.17	0.61	0.20	0.61	0.13	0.6
W2	0.94	29.04	0.04	1.67	0.18	1.67	0.03	0.03	0.28	0.03
W27K	2.64	2.44	2.9	0.12	0.14	0.10	0.01	0.10	0.00	0.14
W30K	2.92	11.15	2.8	2.42	0.07	0.14	0.12	0.22	0.00	0.21
W40K	5.41	16.45	0.04	1.42	0.04	0.13	0.03	16.45	0.00	0.3
W65K	1.09	21.81	0.34	0.45	0.08	0.06	0.01	0.43	0.03	0.01

TABLE 7. Difference in radiant flux results of Pearson Type VII distribution (P7) compared to Gaussian distribution (G) with $n = 2..6$ model functions on the pc-LED set. The following abbreviations are used for the sample: W1=White 1, W2=White 2, WxxK=White xx00K.

LED	$\Delta\Phi$ (%)									
	n=2		n=3		n=4		n=5		n=6	
	P7	G	P7	G	P7	G	P7	G	P7	G
Lime	-0.4	-2.5	0.0	-2.3	0.0	0.3	0.1	-0.3	0.1	-0.1
Purple	-1.3	-3.1	1.2	-2.8	0.0	-0.3	0.1	0.0	0.0	-0.1
W1	0.7	1.3	0.5	-2.8	0.3	-0.2	0.2	-0.2	0.0	0.3
W2	0.9	-0.2	0.1	0.3	0.2	0.3	0.1	0.0	0.3	0.0
W27K	-0.4	0.5	0.4	-0.6	0.2	0.1	0.0	0.1	0.0	0.1
W30K	0.5	-0.2	0.8	0.5	0.1	-0.5	0.0	0.1	0.0	0.1
W40K	1.5	1.4	0.1	1.6	0.1	-0.2	0.1	1.4	0.0	0.1
W65K	1.0	2.0	0.4	-0.1	0.2	-0.1	0.1	0.3	0.1	-0.2

S_2. This allows a tighter fit to the semiconductor emission spectrum. Secondly, a *Gaussian* distribution is a special case of the *Pearson VII* distribution for large exponents $m, S, S_1, S_2 \rightarrow \infty$, thus, it approximates a *Gaussian* distribution at large numerical exponent values and covers the case of *Gaussian* like SPDs. Furthermore, result deviations between both *Pearson VIIa* [4] and *Pearson VIIb* [19] were observed, although both should theoretically yield the same results. The reason can be found in the different types of formulas Reifegerste et al. and Newville et al. provided. While *Pearson VIIb* appears to be the general form of Pearsons Type VII distribution, yet, no information or background on *Pearson VIIa* could be found. Both model functions *Pearson VIIa* and *Pearson VIIb* are shown in (6) and (7) respectively with the Beta-Function $\beta(a,b)$ set to $a = m - b$, $b = 0.5$ and $C = \left[(\lambda - \lambda_p)/\sigma\right]^2$.

$$f_{\mathrm{PVIIa}}(\lambda; A, \lambda_p, \sigma, S) = A \cdot \left[1 + C \cdot \left(2^{\frac{1}{S}} - 1\right)\right]^{-S} \tag{6}$$

$$f_{\mathrm{PVIIb}}(\lambda; A, \lambda_p, \sigma, m) = A \cdot \left[\sigma\beta(a,b)\right]^{-1} \cdot \left[1 + C\right]^{-m} \tag{7}$$

(8)

It should be highlighted, that Reifegerste denotes the parameter S in *Pearson VIIa* and *Split Pearson VII* a "skew"-parameter while the general form of a Pearson Type VII distribution is a symetrical function only providing only a "shape"-parameter m. Moreover, this might give an explanation to some rare cases of *Split Pearson VII* performing slightly worse than *Pearson VIIb* since an accuracy improve-

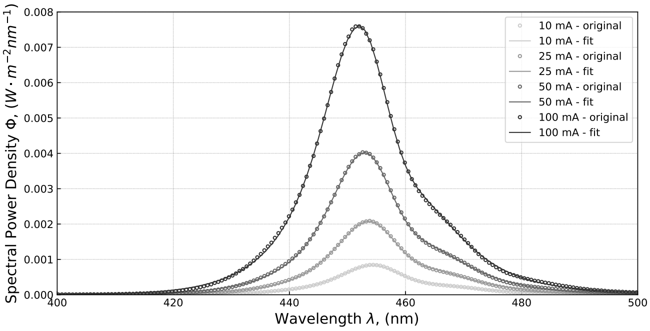

FIGURE 2. Spectral power distribution of a blue monochromatic LED sample for different forward currents I_F: (round markers) Measured SPD and (solid line) fitted SPD with $n = 2$ superimposed *Split Pearson VII* model functions.

ment should be observable due to its left and right side adjustment parameters $\sigma_1, \sigma_2, S_1, S_2$ adding more fit flexibility compared to a non-split *Pearson VIIb* model.

V. APPLICATION EXAMPLE

This section presents an use case of the above proposed *Pearson VII* model for monochromatic LED spectra. Therefore, a spectral measurement of a blue LED (type: Blue 1) at different forward currents of $I_F = [10, 25, 50, 100]\mathrm{mA}$ in an temperature controlled setup was conducted at $T_j \approx 25\,°\mathrm{C}$. This example was specifically chosen due to the unsymmetrical shape of the SPD with a "bump" at around $\lambda \approx 465\,\mathrm{nm}$ to add additional complexity. The measured SPD for each forward current was subsequently fitted with a $n = 2$ function *Split Pearson VII* model. With a $\Delta u'v' \leq 0.001$, $|\Delta\Phi| < 0.2\%$ and $R^2 \geq 0.999$ the applied model yields a very high accuracy for all forward currents. The original SPD and the fitted SPD are shown in figure 2.

Further it should be noted, that the following analysis is intended to show the possibilities and limitations of this approach rather than building a correct physical model. This example evaluates the linear high correlation $|r(I_F, p(I_F))| \rightarrow 1$ indicates a positive or negative linear proportionality between I_F and p. The dependency of each parameter and their linear correlation coefficients are shown in tab. 8 with f_1 and f_2 representing the left and right superimposed functions respectively. The following expectations based on can be evaluated:

TABLE 8. Forward current dependency of *Split Pearson VII* model parameters $p(I_F)$ with two superimposed model functions f_1 and f_2 by means of their correlation $r(I_F, p)$.

Parameter p	$r(I_F, p)$ (a.u.)	
	Function f_1	Function f_2
Amplitude (A)	0.999	0.999
Peak wavelength (λ_p)	-0.986	-0.989
Left side standard deviation (σ_1)	0.997	0.630
Right side standard deviation (σ_2)	0.988	0.992
Left side skew factor (S_1)	0.990	0.611
Right side skew factor (S_2)	-0.107	0.984

1) $I_F \propto A, \sigma_1, \sigma_2$: As more photons are emitted with increasing forward current and thus increasing the SPDs amplitude and thus its standard deviation σ that can be related to the Full Width Half Maximum (FWHM) of the SPD by $FWHM(\sigma) = k\sigma$ where $k = 2\sqrt{2\ln 2}$ in case of a *Gaussian* distribution function [3]. Both functions yield a high correlations for A, σ_1 and σ_2 except σ_1 of f_2. The reason here can be found in the minimal variation of the left split of f_2 since f_2 mainly contributes to shape of the SPDs right side bump.
2) $I_F \propto \lambda_p^{-1}$: With increasing I_F the SPD shifts to lower peak wavelengths λ_p due to piezoelectric field screening [26], [27]. This effect can also be confirmed by both functions parameters λ_p.
3) $I_F \propto S_1, S_2$: Analyzing the shape of the four example spectra three areas are of interest: The SPDs slope left to $\lambda < \lambda_p$ (a), the right sides slope from the SPDs peak to its bump $\lambda_p \geq \lambda_{bump}$ (b) and lastly the right side bumps prominence (c). Regarding the parameter S_1 table 8 shows a high correlation for f_1 and a mediocre correlation for f_2 since f_1 mainly affects above described area (a). Similar, f_2 controls the areas and (c) by the parameter S_2. The low correlation of functions f_1 parameter S_2 occurs since the fit algorithm tries to model the right split of f_1 to fit around the bump modeled by f_2. This point clearly shows potential for optimization. One solution can be implementing so called expression models for each parameter to follow a certain physical function.

VI. CONCLUSION AND FUTURE WORK

In this work the least squares fitting performance of different probability density model functions on monochromatic and phosphor-converted LED spectra was evaluated. A total of 19 different model functions was examined with $n = 1..3$ and $n = 2..6$ superimposed functions of the same type on seven monochromatic and eight pc-LED spectra respectively. A literature research demonstrated that the coefficient of determination as a goodness of fit metric has a low information value since an $R^2 \geq 0.95$ for the majority of cases was reported. A combination of the change in chromaticity $\Delta u'v'$ and radiant flux $\Delta\Phi$ as well as the Bayesian Information Criterion proved to be more meaningful in mathematical terms and also in accordance with the human light perception. As a key result it was concluded that a *(Split) Pearson VII* model function yields highly accurate results on the evaluated SPD sample set contrary to the commonly used *Gaussian* model function. A promising usability of a *(Split) Pearson VII* distribution to model the current dependency of a blue LED was furthermore presented. Thus, this works recommends the *(Split) Pearson VII* model function for the purpose of spectral modeling and decomposition. However, in this work a globally set of fit parameter constraints was applied to all functions. Fitting results may be further improved by determining model specific constraints and starting parameters. As discussed before the origin of difference of the three Pearson Type VII model functions *VIIa, VIIb, Split VII* has to be examined in depth.

VII. ACKNOWLEDGMENTS

This project has received funding from the ECSEL Joint Undertaking (JU) under grant agreement No 101007319. The JU receives support from the European Union's Horizon 2020 research and innovation programme and Netherlands, Hungary, France, Poland, Austria, Germany, Italy, Switzerland. The work reported in this paper reflects the author's view and that the JU is not responsible for any use that may be made of the information it contains.

REFERENCES

[1] "CIE 015:2018 Colorimetry, 4th Edition," Oct. 2018.

[2] S. Benkner, S. Babilon, A. Herzog, and T. Q. Khanh, "Combined Methodology for Accurate Evaluation of Distance and Direction of Chromaticity Shifts in LED Reliability Tests," *IEEE Transactions on Device and Materials Reliability*, vol. 21, no. 4, pp. 500–507, Dec. 2021.

[3] E. F. Schubert, *Light-Emitting Diodes*, 2nd ed. Cambridge: Cambridge University Press, 2006.

[4] F. Reifegerste and J. Lienig, "Modelling of the Temperature and Current Dependence of LED Spectra," *Journal of Light & Visual Environment*, vol. 32, no. 3, pp. 288–294, 2008.

[5] R. Supronowicz and I. Fryc, "The LED spectral power distribution modelled by different functions - how spectral matching quality affected computed LED color parameters," in *2019 Second Balkan Junior Conference on Lighting (Balkan Light Junior)*, Sep. 2019, pp. 1–4.

[6] A. Keppens, W. R. Ryckaert, G. Deconinck, and P. Hanselaer, "Modeling high power light-emitting diode spectra and their variation with junction temperature," *Journal of Applied Physics*, vol. 108, no. 4, p. 043104, Aug. 2010.

[7] M. E. Raypah, M. Devarajan, and F. Sulaiman, "Modeling Spectra of Low-Power SMD LEDs as a Function of Ambient Temperature," *IEEE Transactions on Electron Devices*, vol. 64, no. 3, pp. 1180–1186, Mar. 2017.

[8] D. Mozyrska and I. Fryc, "Approximation of spectroradiometric data by fractional model," *Przeglad Elektrotechniczny*, vol. 87, Feb. 2011.

[9] A. Vaskuri, H. Baumgartner, P. Kärhä, G. Andor, and E. Ikonen, "Modeling the spectral shape of InGaAlP-based red light-emitting diodes," *Journal of Applied Physics*, vol. 118, no. 20, p. 203103, Nov. 2015.

[10] A. Vaskuri, P. Kärhä, H. Baumgartner, O. Kantamaa, T. Pulli, T. Poikonen, and E. Ikonen, "Relationships between junction temperature, electroluminescence spectrum and ageing of light-emitting diodes," *Metrologia*, vol. 55, no. 2, pp. S86–S95, Mar. 2018.

[11] Z. Guo, T. Shih, Y. Gao, Y. Lu, L. Zhu, G. Chen, Y. Lin, J. Zhang, and Z. Chen, "Optimization Studies of Two-Phosphor-Coated White Light-Emitting Diodes," *IEEE Photonics Journal*, vol. 5, no. 2, pp. 8 200 112–8 200 112, Apr. 2013.

[12] B.-M. Song and B. Han, "Spectral power distribution deconvolution scheme for phosphor-converted white light-emitting diode using multiple Gaussian functions," *Applied Optics*, vol. 52, no. 5, p. 1016, Feb. 2013.

[13] W. Chen, J. Fan, C. Qian, B. Pu, X. Fan, and G. Zhang, "Reliability Assessment of Light-Emitting Diode Packages With Both Luminous Flux Response Surface Model and Spectral Power Distribution Method," *IEEE Access*, vol. 7, pp. 68 495–68 502, 2019.

[14] H. Chen and S. Y. Hui, "Dynamic Prediction of Correlated Color Temperature and Color Rendering Index of Phosphor-Coated White Light-Emitting Diodes," *IEEE Transactions on Industrial Electronics*, vol. 61, no. 2, pp. 784–797, Feb. 2014.

[15] J. Fan, M. G. Mohamed, C. Qian, X. Fan, G. Zhang, and M. Pecht, "Color Shift Failure Prediction for Phosphor-Converted White LEDs by Modeling Features of Spectral Power Distribution with a Nonlinear Filter Approach," *Materials*, vol. 10, no. 7, p. 819, Jul. 2017.

[16] J. Fan, W. Chen, W. Yuan, X. Fan, and G. Zhang, "Dynamic prediction of optical and chromatic performances for a light-emitting diode array based on a thermal-electrical-spectral model," *Optics Express*, vol. 28, no. 9, pp. 13 921–13 937, Apr. 2020.

[17] J. Fan, Y. Li, I. Fryc, C. Qian, X. Fan, and G. Zhang, "Machine-Learning Assisted Prediction of Spectral Power Distribution for Full-Spectrum White Light-Emitting Diode," *IEEE Photonics Journal*, vol. 12, no. 1, pp. 1–18, Feb. 2020.

[18] C. Qian, J. Fan, X. Fan, and G. Zhang, "Prediction of Lumen Depreciation and Color Shift for Phosphor-Converted White Light-Emitting Diodes Based on A Spectral Power Distribution Analysis Method," *IEEE Access*, vol. 5, pp. 24 054–24 061, 2017.

[19] M. Newville, T. Stensitzki, D. B. Allen, and A. Ingargiola, "LMFIT: Non-Linear Least-Square Minimization and Curve-Fitting for Python," Zenodo, Sep. 2014.

[20] H.-T. Chen, W. C. H. Choy, and S. Y. Hui, "Characterization, modeling, and analysis of organic light-emitting diodes with different structures," *IEEE Transactions on Power Electronics*, vol. 31, no. 1, pp. 581–592, Jan. 2016.

[21] X. Shen, H. Chen, J. Lin, Y. Li, H. Lin, J. Chen, and C. Chen, "Analysis and Modeling of Optical and Thermal Properties of Phosphor Converted White Light Emitting Diode," *IEEE Access*, vol. 7, pp. 118 679–118 689, 2019.

[22] G. Schwarz, "Estimating the Dimension of a Model," *The Annals of Statistics*, vol. 6, no. 2, pp. 461–464, Mar. 1978.

[23] W. Hu and W. Davis, "Dimming curve based on the detectability and acceptability of illuminance differences," *Optics Express*, vol. 24, no. 10, pp. A885–A897, May 2016.

[24] "CIE TN 001:2014: Chromaticity Difference Specification for Light Sources," 2014.

[25] "ANSI/IES TM-35-19+E1, Technical Memorandum: Projecting Long-Term Chromaticity Coordinate Shift of LED Packages, Arrays, and Modules," 2019.

[26] H. Itoh, S. Watanabe, M. Goto, N. Yamada, M. Misra, A. Y. Kim, and S. A. Stockman, "Current Dependence of In-Plane Electroluminescence Distribution of $In_xGa_{1-x}N$/GaN Multiple Quantum Well Light Emitting Diodes," *Japanese Journal of Applied Physics*, vol. 42, no. Part 2, No. 10B, pp. L1244–L1247, Oct. 2003.

[27] A. Herzog, M. Wagner, and T. Q. Khanh, "Efficiency droop in green InGaN/GaN light emitting diodes: Degradation mechanisms and initial characteristics," *Microelectronics Reliability*, vol. 112, p. 113792, Sep. 2020.

SIMON BENKNER received his B.Sc. and M.Sc. in electrical engineering in 2015 and 2017 from Technical University of Darmstadt, Germany. As of today he is working as a Research Assistant and Ph.D. candidate at the Laboratory of Adaptive Lighting Systems and Visual Processing at Technical University of Darmstadt. His research interests focuses on the reliability analysis of light-emitting diodes by applying physical and data driven models to increase lifetime prediction accuracy. In addition he engages in research on smart lighting systems and digital twins in the context of lighting applications.

ALEXANDER HERZOG was born in Offenbach, Germany, in 1987. He received his B.S., M.S. and Ph.D. degree in electrical engineering in 2012, 2015 and 2020 from Technical University of Darmstadt. Currently he works as a Postdoctoral researcher at the Laboratory of Adaptive Lighting Systems and Visual Processing at Technical University of Darmstadt. Dr. Herzog's research interests include lifetime prediction, reliability analysis and digital twins of light-emitting diodes. Additional research topics are temporal light artefacts and spectral optimization of metameric spectra.

STEFAN KLIR M. Sc., received his M. Sc. degree in the field of Electrical Engineering and Information Technology from the Technical University of Darmstadt, Germany, in 2017. He is currently pursuing his Ph.D. at the Laboratory of Adaptive Lighting Systems and Visual Processing, Technical University of Darmstadt, Germany. His research is focused on the development of intelligent, data-driven lighting control systems for integrative lighting applications and to enhance individual user preference.

WILLEM D. VAN DRIEL graduated as a mechanical engineering at Technical University of Eindhoven and received a PhD degree from Delft University of Technology, the Netherlands. He has a >25 year track record in the reliability domain. Application areas range from healthcare, gas and oil explorations, semiconductors. His current position is Fellow Scientist at Signify (formerly Philips Lighting). Besides that, he holds a professor position at the University of Delft, The Netherlands. His scientific interests are solid state lighting, microelectronics and microsystems technologies, virtual prototyping, virtual reliability qualification and designing for reliability of microelectronics and microsystems. He is chair of the organizing committee of the IEEE conference EuroSimE. He has authored and co-authored more than 350 scientific publications, including journal and conference papers, book or book chapters and invited keynote lectures.

TRAN QUOC KHANH received the Dr.-Ing. degree in physics and technology of electronic components and the Habilitation degree in mechanical engineering and technical optics from the Institute for Lighting Technology at Technical Univerity of Illmenau, Germany, in 1989 and 2005, respectively. Since 2006, he has been a Full Professor and the Head of the Laboratory of Adaptive Lighting Systems and Visual Processing, Technical University of Darmstadt, where he has served as the Dean for the Department of Electrical Engineering and Information Technology since 2018. He leads research groups in the field of automotive lighting, human-centric lighting, smart indoor lighting, and LED technology.